Smithsonian
Museum Conservation Institute

Requested Report **MCI #6304**

BIOCOLONIZATION OF THE NMAI BUILDING AND IMAGE ANALYSIS METHODS FOR ITS EVALUATION

Eric May, Robert Inkpen, and Christine Hughes

Eric May, *Reader in Microbiology*
School of Biological Sciences, University of Portsmouth,
King Henry I Street, Portsmouth PO1 2DY, Hampshire, United Kingdom
e-mail eric.may@port.ac.uk

Robert Inkpen, *Reading in Physical Geography*
Department of Geography, University of Portsmouth,
Buckingham Building, Lion Terrace,
Portsmouth, Hampshire PO1 2HE, United Kingdom

Christine Hughes
School of Biological Sciences, University of Portsmouth,
King Henry I Street,
Portsmouth PO1 2DY, Hampshire, United Kingdom

November 2010

Introduction

Microalgae and cyanobacteria are common colonisers of stone of buildings and monuments in different climates throughout the world; reports of their diversity are available from Europe (Macedo et al., 2009), Asia (Samad and Adhikary, 2008), and South America (Crispim and Gaylarde, 2005; Crispim et al., 2006). Rindi (2007) reviewed the diversity of green algae and cyanobacteria in urban habitats and highlighted how limited our knowledge is in this field.

At the invitation of the Museum Conservation Institute, a group of interested researchers from the U.K., Germany, and Italy participated in a workshop and visited the museum during April 2010 to consider the nature and causes of the staining. Samples were removed during the visit and taken back to individual laboratories for analysis. This report is a summary of investigations undertaken at the University of Portsmouth in the Schools of Biological Sciences and Geography. The paper focuses on identifying the biological basis of the discoloration and on analysing the images of surface discoloration. Image analysis is being increasingly used in the identification and quantification of stone decay (e.g., Inkpen et al., 2008; Thornbush and Viles, 2006) and this paper adds to this literature by introducing a method for quantifying variations in the spatial patterns of discoloration across a number of scales.

Experimental Approach

Four samples were considered:

- Sample #2 is a small stone fragment from the first course of the low wall by the loading dock at the north-west corner of the NMAI building.
- Sample #7 is a small stone fragment from the east facing wall below the scupper on the roof beyond the Senator Daniel K. Inouye Terrace.
- Sample #9 is slime material from 6th floor roof runoff scraped from membrane found under the masonry by the 5th floor scupper near the Inouye Terrace.
- Sample #10 is a stone block of the same Kasota limestone from spare blocks not used in the building that were stored outdoors. The block had the exposed weathered face with a blackish appearance similar to the other two samples.

The following methods were used to evaluate the nature of the black stains on the stone samples:

Light microscopy: The surfaces of the stained samples were examined directly with a light stereo-microscope at low magnification. Small sub-samples of #2 were scraped from the stained area and suspended in sterile water on a glass microscope slide, and observed using a compound light microscope at different magnifications. Scupper slime samples (#9) were suspended directly in water and also observed by light microscopy.

Scanning Electron Microscopy (SEM): Sample #2, from the N.W. corner wall, was fixed in glutaraldehyde, dehydrated in an alcohol series, sputter coated, and examined with a Joel scanning electron microscope.

Enrichment culture: Samples were scraped from sample #7 and suspended in Bold's Basal Medium (a mineral-based medium for growth of photosynthetic microorganisms) and incubated in a white light illuminated incubator at 28°C until growth was evident. This was initially unsuccessful so the procedure was repeated 3 times until growth was obtained.

Image analysis: The stained surface of a stone block (#10) was analysed by image analysis using a combination of a commercial photographic manipulation software and specialist image analysis software (ERDAS IMAGINE) in order to determine the nature of the distribution of the surface discoloration.

Light microscopy

Stereo light microscopy showed that the black stain on sample #2 was unevenly distributed in small black clumps or tufts over the stone surface (Figure 1a). The small clumps were readily removed by scraping and could be suspended in water and observed under light at low magnification (Figure 1b).

These clumps were composed of filaments that protruded from the main mass of the clump (Figure 1c), and these were seen more clearly under higher magnification (Figure 1d). Delicate pressure on the coverslip over the specimen caused the clumps to disaggregate and the filaments were released (Figure 1e-1f).

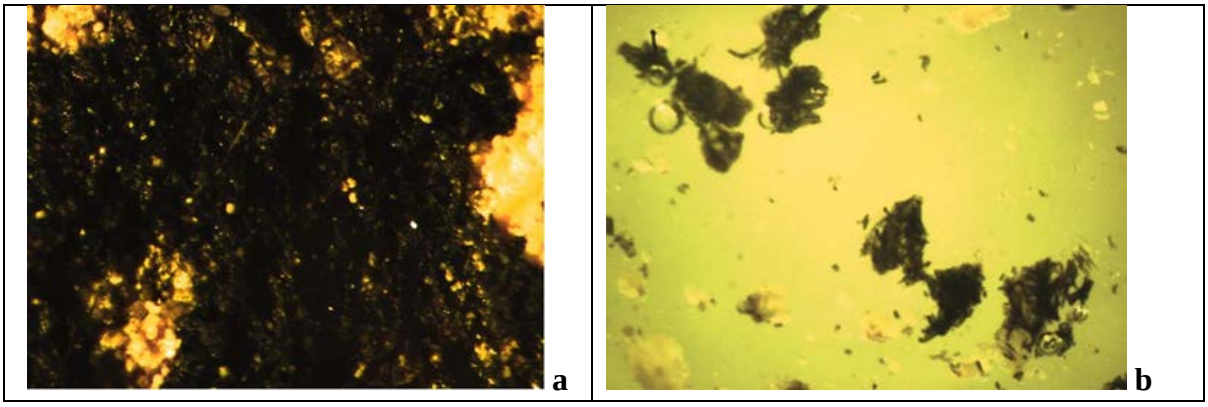

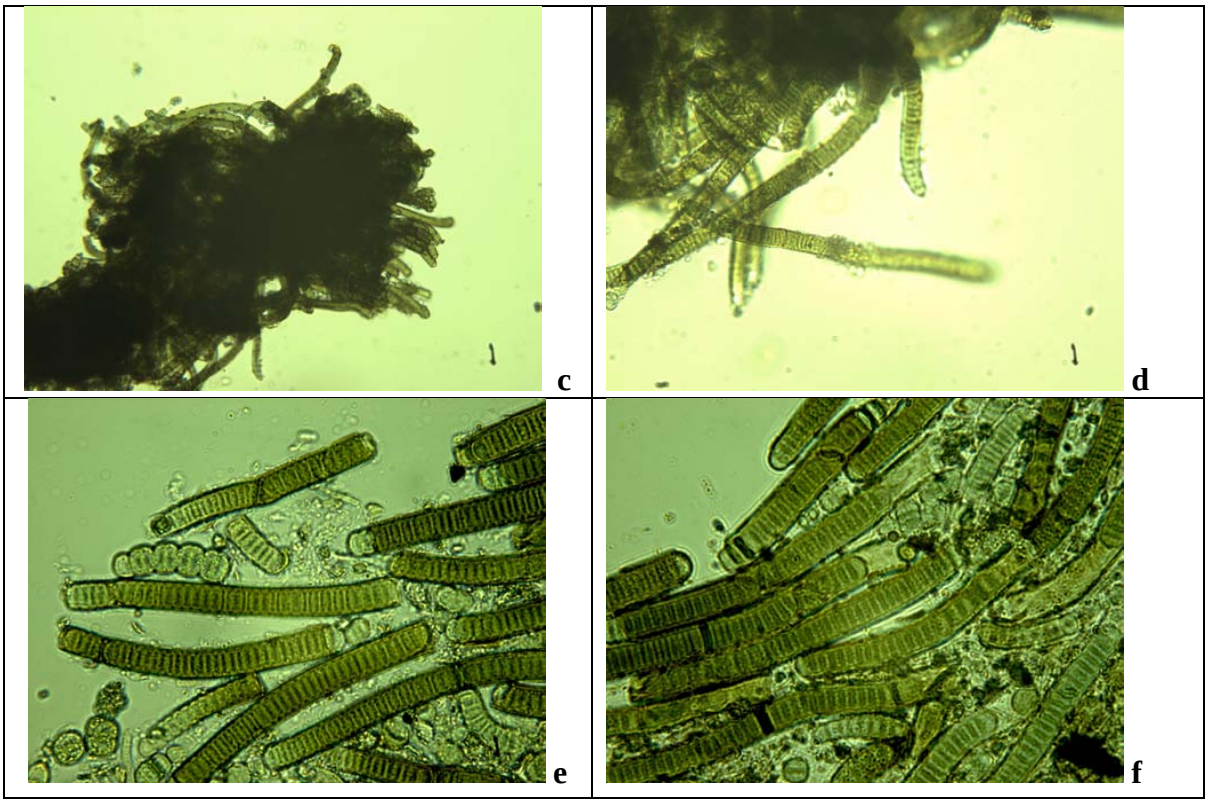

Figure 1. (a) Examination of the black stained stone surface (sample #2) under white light using low power stereomicroscope (30x). (b) Surface scrapings were suspended in water on a slide and black clumps were observed (45x). (c) The black clumps are composed of masses of green filaments (200x). (d) These filaments protrude from the center. (e)-(f) Two views of their clear cellular structure within an outer sheath (400x).

The component flora was a mixed community but the dominant type was a filamentous photosynthetic alga, about 7.5 μm wide, which appeared to be present within an external brown sheath. The dark colour of the stain appeared to be caused by dense packing of the brown-sheathed filaments or trichomes. The filaments had rounded ends and were composed of short green cells about 2-3 μm long. Filaments consisted of variable numbers of cells but usual not less than 10 cells. No branching was seen. Other types of cells were present but their numbers were small compared with the dominant filamentous alga.

Examination of the slime removed from the membrane below the roof scupper (Sample #9) also showed a tuft/clump structure with filamentous organisms embedded in a slime matrix but the cellular arrangement was not as obvious within the filaments (Figure 2a-c). This may have been due to the fact that this examination did not take place until the samples were already some weeks old. Nevertheless, the analysis reveals that the slime balls obtained from the scupper were composed as the same organism as the surface stains on the stone blocks.

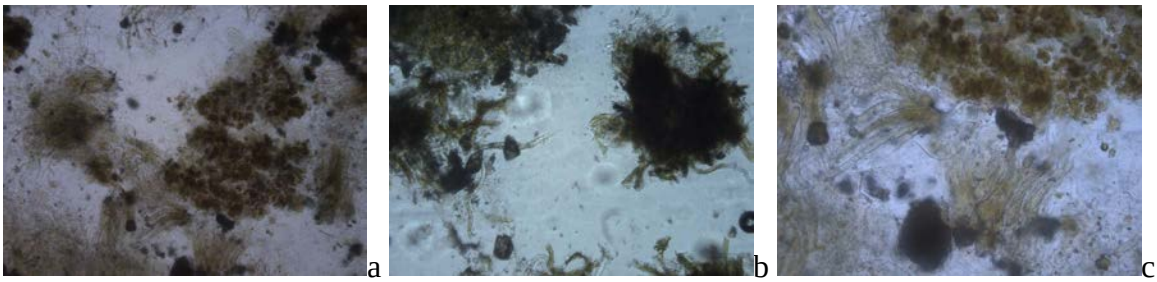

Figure 2. Examination of material removed from the membrane below the area of the roof scupper (sample #7). (a) and (b) show black clumps of slime infiltrated by complex mixed population with protruding filaments (both x 100). (c) Higher-power view of filamentous growth (~7 μm width, x 200).

A number of sources were consulted in order to identify the type and genus of the dominant organism causing the contamination (Tomaselli et al., 2002; John et al., 2002; Crispim and Gaylarde, 2005; Samad and Adhikary, 2008; Macedo et al., 2009). The colour, size, and morphology suggest that the organism is a non-heterocystous cyanobacterium, a member of the Order Oscillatoriales and probably a member of the genera *Oscillatoria* or *Lyngbya*. It is difficult to be precise about the species name but taking all the morphological and ecological evidence together it could be *Oscillatoria nigra* or *Lyngbya martensiana*. Definitive identification would require molecular analysis of DNA.

Electron microscopy

Stone samples (#2) from the N.W. corner of the loading dock wall were analysed by SEM. The stone had been subject to repeated wetting and drying and exposure to daylight over a period of 2 months to maintain the black stain. This analysis showed that the black stained zone was covered in filamentous masses (Figure 3a) composed of strands of varying widths but dominated by strands about 7-10 μm wide (Figure 3b). The cut sound face of the sample showed no such growths (Figure 3c).

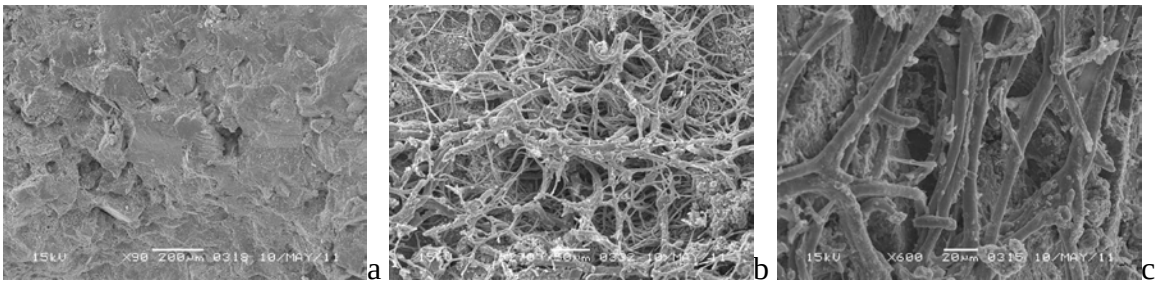

Figure 3. Appearance of black stained zone from sample #2 by scanning electron microscopy. (a) Sound cut stone face. (b) Filamentous growth on the black zone. (c) Showing that filament diameter (~7.5 μ) is similar to that observed by light microscopy.

Enrichment Culture

The stone sample (#7) from below the scupper was scraped to remove small fragments of stone and the black stain, which were added to sterile Bold's Basal Medium, a mineral medium to support the growth of photosynthetic microbes, in a 100 mL conical flask. The flask was incubated in an illuminated incubator at 28°C until growth was evident. This did not occur over a 4-week period. It was repeated on 2 further occasions until eventually the flask contents showed clear signs of green algal growth. Samples from the flask were observed under light microscopy. The original stone clumps were still visible in the culture medium (Figure 4a) and large amounts of filamentous growth could be seen protruding from the stone masses. At higher magnification (Figure 4b), these filaments were shown to be of different thickness, indicating the presence of a mixed community. Planktonic species of both unicellular and filamentous algae were also seen to be present in the bulk liquid of the culture, but the culture consisted mostly of filamentous types. One of the dominant filamentous types, especially associated with the stone particles, was a cyanobacterial trichome similar to those that had been found on the original blackened stone zone. The filaments were about 7 μm wide and divided into short cells and forming long, unbranched filaments that did not contain heterocysts (Figure 4c). Thus although the culture had supported the growth of the original dominant filamentous microbe, other organisms had grown.

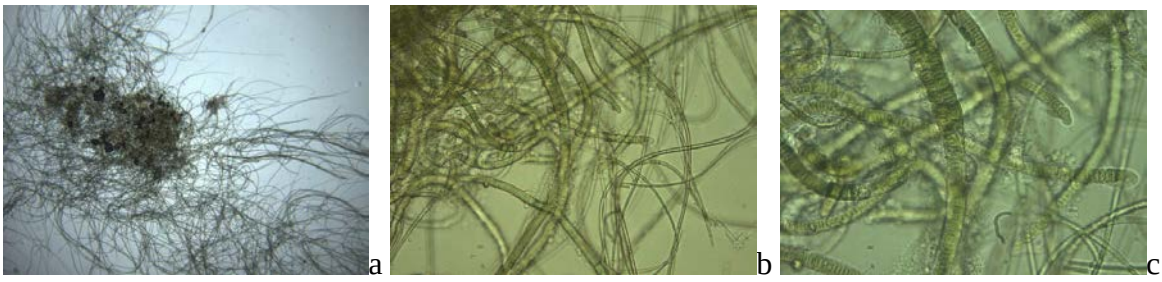

Figure 4. Growth after culture of sample #7 in Bold's Basal Medium (BBM) showing: (a) Stone clumps with original black stain showing extensive filamentous growth (x 40); (b) Several types of green pigmented filaments of varying diameter (x 200): and (c) Under high-power (400x) cyanobacterial filaments, as seen in the original light micrographs immediately after removal from the NMAI *building.*

Image Analysis

The surface of the sample (#10) provided was relatively flat and so it was felt that laser scanning would yield few interesting variations. Instead image analysis of the sample was undertaken using a combination of a commercial photographic manipulation software and specialist image analysis software (ERDAS IMAGINE). The purpose of undertaking image analysis was to explore the nature of the distribution of the surface discoloration. Specifically analysis focused on two questions:

1. Did the amount of surface discoloration change as the intensity of discoloration was varied?

2. Did the spatial distribution of surface discoloration alter as the scale of observation altered?

The first question considered the degree or intensity of discoloration – how blackened the surface was and if considering this aspect of discoloration helped in identifying patterns on the surface. The second question considered if there was any pattern to discoloration of a certain degree or intensity. As the scale of observation changes it might be expected that discoloration will become more pronounced in some areas and less so in others if there is a factor or set of factors concentrating discoloration into distinct zones on the surface.

The sample surface was scanned using a photogrammetric scanner at a pixel resolution of 20 microns. The scanner was set on a bright setting and a single moving light source illuminated the sample to ensure that the surface was given the same intensity of lighting for the scan. No other manipulation of the image was carried out and Figure 5 shows the image that formed the basis for further analysis. The image was saved and analysed as a TIFF file to ensure that no information was lost in a compression process as would occur with a JPEG format. The resulting image records a value for each pixel of between 0 and 255, 0 being black and 255 being white.

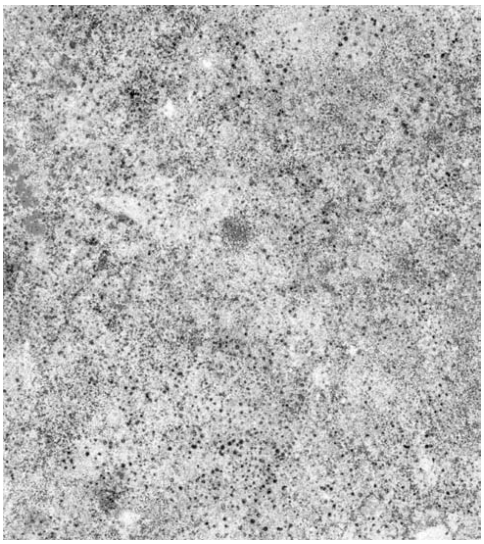

Figure 5. Scan of sample (#10) surface at 20 μm resolution.

This image was then transferred to a photo manipulation package and a series of images produced based on setting a threshold value. Setting a threshold value classifies the pixels in the image into one of two classes, either above or below the threshold. If the pixel value is above the threshold they are recorded as black – a pixel value of 0 – if pixels are below the threshold they are recorded as white – a pixel value of 255. Figures 6a-h provide illustrations of the scanned surface at different threshold values. This means that the proportion of the image classified as 'blackened' for a particular threshold can be quantified by counting the number of pixels in that class and dividing by the total number of pixels in the whole image.

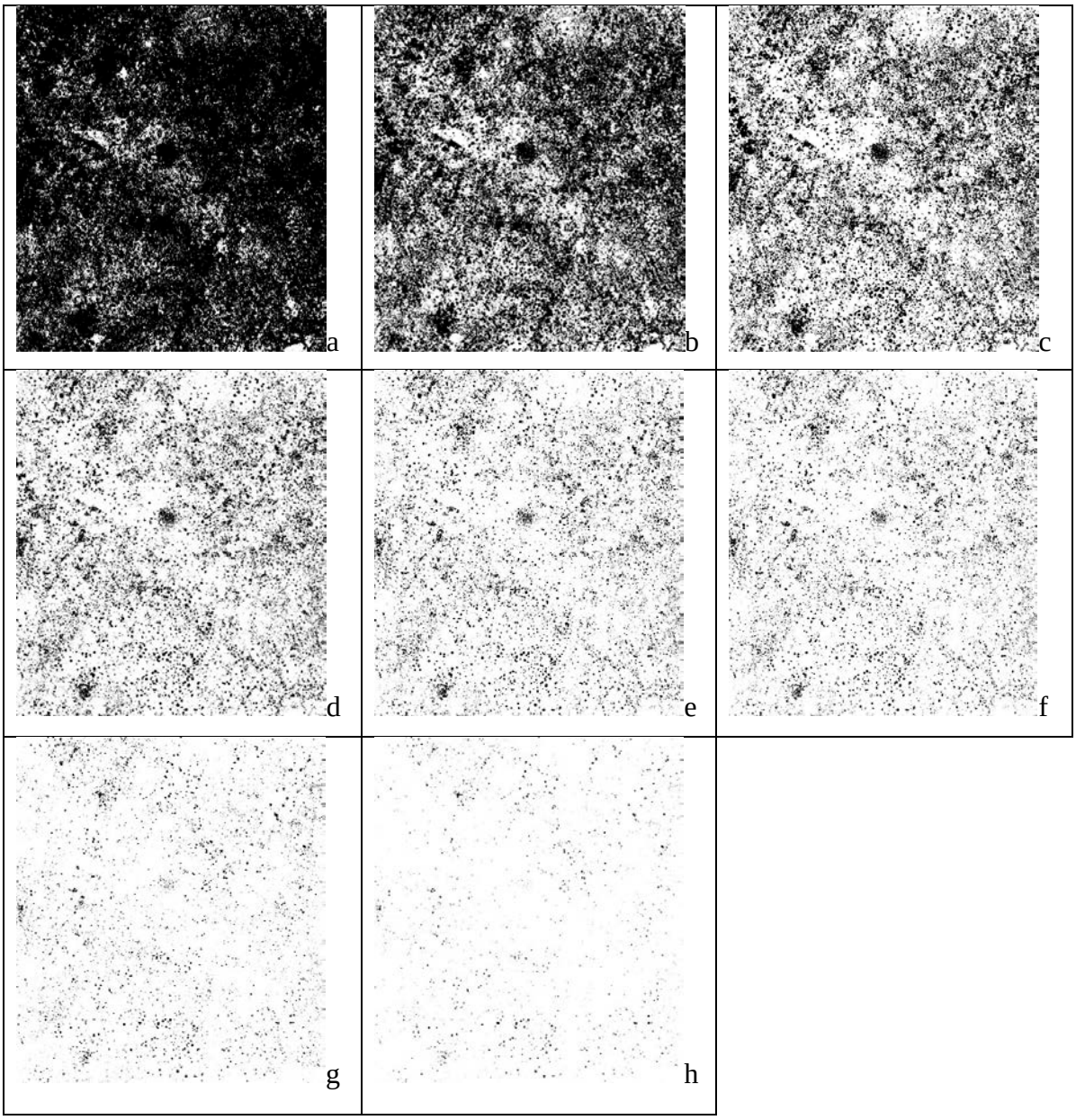

Figure 6. Scan of surface of sample #10 at different threshold values. (a) 225, the highest value; (b) 200; (c) 175; (d) 150; (e) 130, the image used for analysis of the spatial variability of the distribution of surface blackening. (f) 125; (g) 100; (h) 75.

Figure 7 illustrates how the proportion of the same areas classed as 'blackened' decreases dramatically at a pixel value of around 150. This suggests that above this threshold the discoloration of the surface may be a result of general dust and particulate deposition. Below this threshold value, the blackened areas are more disconnected and seem to be circular or clumps of discoloration implying that deposition of this surface discoloration is more localized and potentially controlled by surface-specific factors.

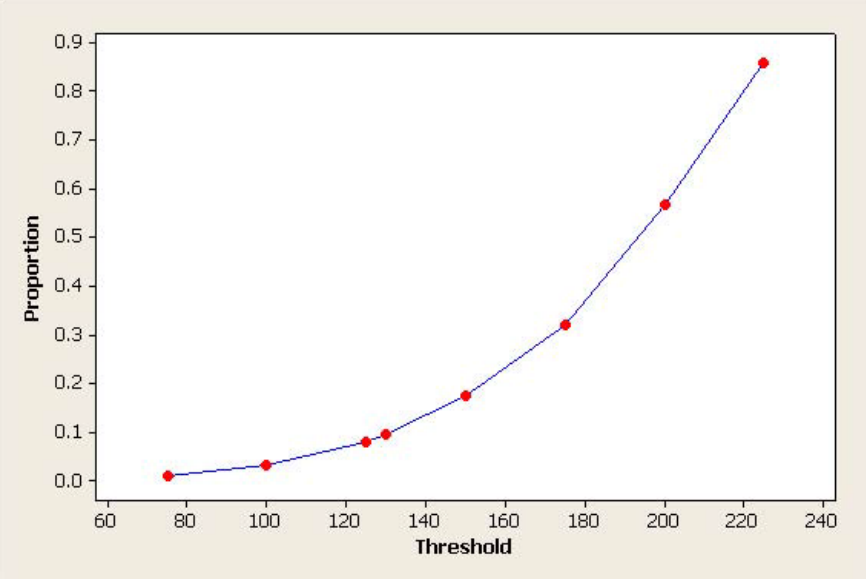

Figure 7. Change in proportion of surface classified as 'blackened' as threshold value changes.

The spatial distribution of discoloration was assessed by dividing the sample into increasingly small units and calculating the proportion of blackened to white pixels in each cell. The division process was as in Figure 8. This is a variant of the box counting process method used to identify fractal dimensions of patterns (Buczkowski et al., 1998, Dathe et al., 2001). The process produced 1 large cell, the whole surface with an area of approximately 2000 mm^2, 4 cells with an area of 400mm^2 each, 16 cells with an area of 100 mm^2 each and 64 cells with an area of 25 mm^2 each. (Please note that to aid division of the surface within ERDAS IMAGINE a small area of the surface section was excluded from analysis). As this was a labour-intensive and time-consuming process this form of analysis was only carried out for a single threshold value of 130 but it could be carried out for other threshold values if specific patterns of interest can be identified for a particular level of surface blackening or threshold value.

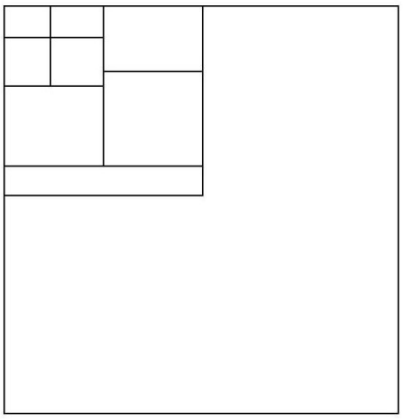

Figure 8. Division of scanned image into cells of decreasing size illustrated in top left hand corner of figure.

Figure 9 illustrates the relationship between the proportion of the surface blackened and the size of the cell considered (a log scale is used to enable easier visual comparison of cell sizes). The graph does suggest that as the size of the cell decreases the variability of the proportion of the surface blackened increases. At the smallest cell size considered, cells with an area of 25 mm^2, the range of values is from 0.03 to 0.28, but it is important to note that the mean proportion blackened remains consistent at 0.11 at all scales.

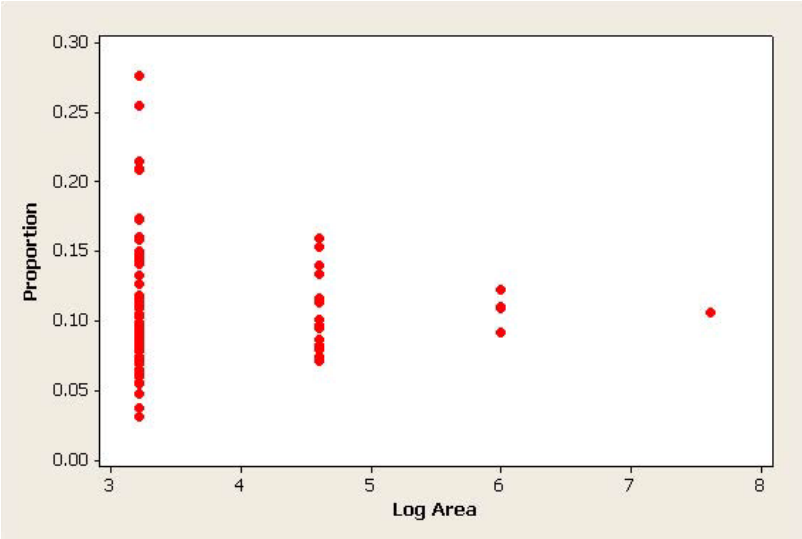

Figure 9. Plot of log of area of cells against proportion of surface blackened in cells of that area at the threshold value of 130.

Figure 10 highlights that the range of values increases steeply but also steadily as the scale of the cells considered changes implying a consistent pattern to the surface cover.

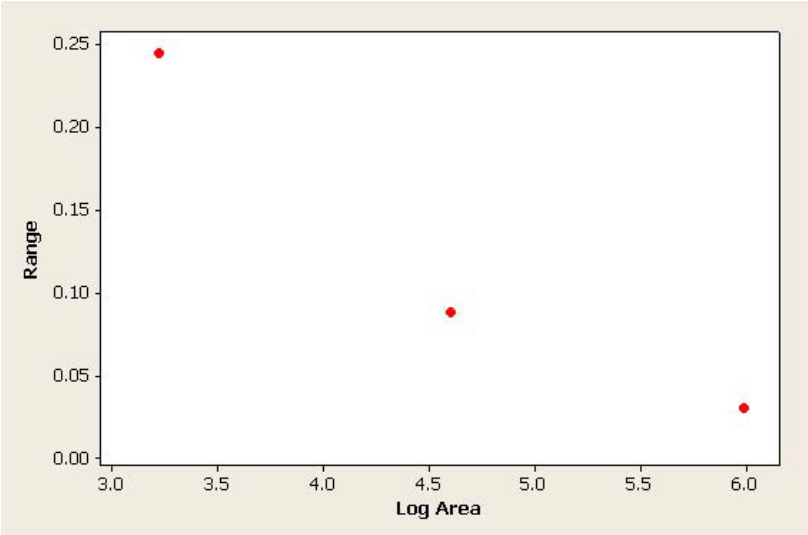

Figure 10. Plot of the log area of cells against the range of the proportion of surface area blackened for cells of that area at a threshold value of 130.

The histograms in Figures 11 and 12 also illustrate that despite the increasing variability of the proportions of the surface covered, there is still a single peak to the histogram at these two scales. For the cells of 100 mm^2, there is a suggestion of a bi-modal distribution but not into cells with no blackening and cells with a lot of blackening but rather into lightly and heavily blackened cells. For cells of 25 mm^2 in area there is a clear single peak but with a tail of heavily blackened cells. This suggests that there may be a factor influencing the spatial distribution of the degree of blackening at the scale of 100 mm^2 and that a factor operating at the scale of 25 mm^2 may be producing a tail of heavily blackened cells but there is little evidence of a clear, distinct scale-dependent variation in the proportion of the surface blackened at the scales considered in this analysis. This would imply that the spatial distribution of the blackening, at the threshold value selected, is relatively homogeneous at the scales of cells considered.

It is possible that this box counting method could be applied at the scale of the whole wall or even building to compare how the spatial distribution changes with scale. The number of images required, however, to cover a wall or building at the highest resolution would be impractical to analyse. It might be possible, however, to have a hierarchical, nested sampling strategy where images at a relatively low resolution were used to photograph the whole wall or building. Analysis of these images would be able to identify areas of spatial diversity and these could be the focus for higher resolution imagery. This could enable researchers to match decay processes at specific scales with spatial variations in decay forms such as discoloration, over a range of scales.

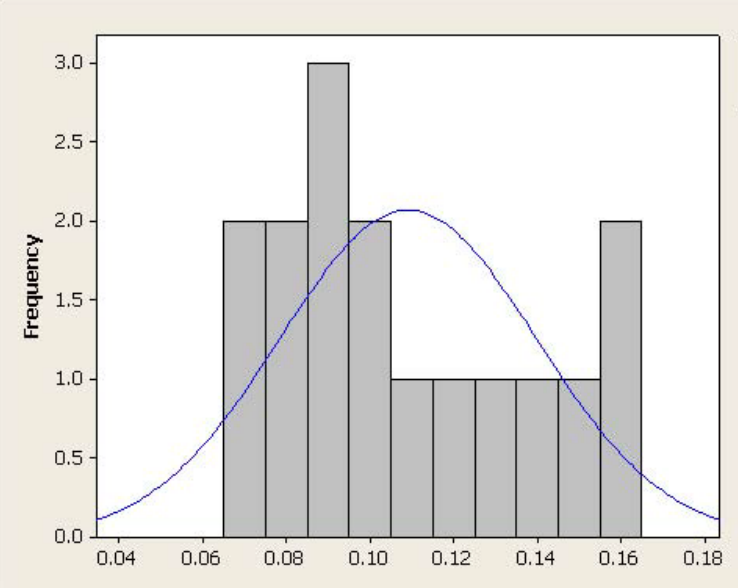

Figure 11. Frequency plot of proportion of surface area of cell blackened at threshold of value 130 for cells 100 mm^2 in area (Mean=0.1091; StDev=0.03083; N=16).

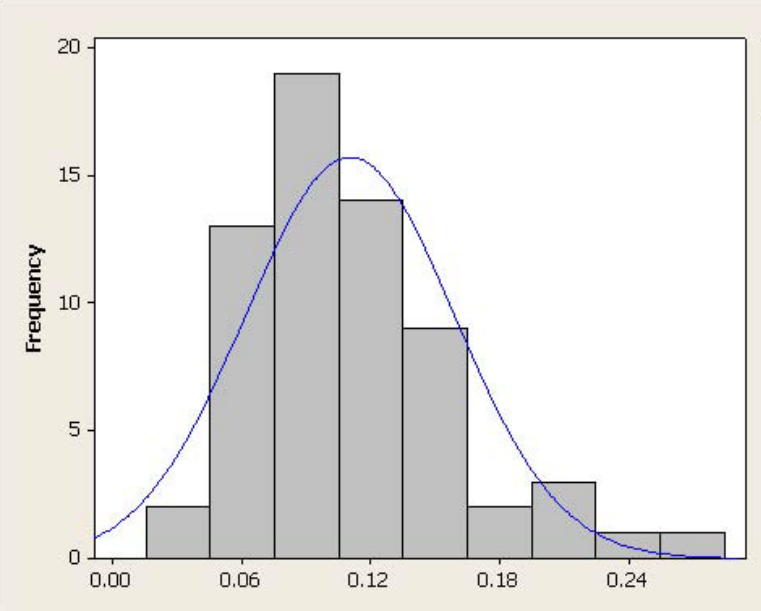

Figure 12. Frequency plot of proportion of surface area of cell blackened at threshold of value 130 for cells 25 mm² in area (Mean=0.1103; StDev=0.04879; N=64).

Conclusions

Analysis showed the black-stained zone of the Kasota limestone to be primarily due to growth of tuft-forming filamentous blue-green algae, which form trichomes due to a brown sheath covering the blue-green cyanobacterial filaments. These were observed by light and electron microscopy. These organisms form dense brown to black clumps that are readily observed on the surface of the stone. Similar organisms are commonly found by other researchers on buildings in temperate and tropical climates. The original community in the black zones was a mixed community but the dominant type was a filamentous cyanobacterial type, probably belonging to the Order Oscillatoriales, and with a cell and filament morphology ressembling *Oscillatoria* or *Lyngbya.* The very dark nature of the growth suggests that it could be *Oscillatoria nigra* but it could also be *Lyngbya martensiana* due to its growth habit. The dominant organism did eventually grow in laboratory culture but the enrichment procedure was not straightforward and a complex mixed culture was obtained. Image analysis of the distribution of the black zone showed that it was evenly distributed although the visual evidence obtained by microscopy showed that growth occurred in small but evenly distributed clumps over the face of the stone. The reason for this is that image analysis simulates our appreciation of soiling on architectural surfaces, where soiling appears fairly homogeneous. This approach is similar to that developed by Charola et al. (2012)* that can be applied to larger surfaces and can be used to monitor and evaluate the effectiveness of cleaning methods or applied biocides. Furthermore, although the size and distribution of the black 'spots' in the images is at a different scale from the distributions highlighted in the photomicrographs, the two distributions may be related, with the

black spots in the images reflecting the aggregation of individual organic entities to form localised observable accumulations. These local concentrations of material then produce the spatial patterns observed in the image analysis. The variability of these patterns at the smaller spatial scale reflects the importance of micro-scale variations, observed in the photomicrographs, and their translation to the observable entities in the images.

*****_Minor changes were made to this report, such as inclusion of this reference._

References

Buczkowski, S., S. Kyriacos, F. Nekka, and L. Cartllier. 1998. The modified box-counting method: analysis of some characteristic parameters. *Pattern Recognition*, 31:411-418.

Charola, A. E., M. Wachowiak, E. Keats Webb, C. A. Grissom, E. P. Vicenzi, W. Chong, H. Szczepanowska, and P. T. DePriest. 2012. "Developing a Methodology to Evaluate the Effectiveness of a Biocide." In *Proceedings 12th International Congress on Stone Deterioration and Conservation*. Available on line at http://iscs.icomos.org/cong-12.html (accessed June 10, 2015).

Crispim, C.A., and C. C. Gaylarde. 2005. Cyanobacteria and Biodeterioration of Cultural Heritage: A Review. *Microbial Ecology*, 49:1-9.

Crispim, C.A., P. M. Gaylarde, C. C. Gaylarde, and B. A. Neilan. 2006. Deteriogenic Cyanobacteria on Historic Buildings in Brazil Detected by Culture and Molecular techniques. *International Biodeterioration and Biodegradation*, 57:239-243.

Dathe, A., S. Eins, J. Niemeyer, and G. Gerold. 2001. The Surface Fractal Dimensions of the Soil-pore Interface as Measured by Image Analysis. *Geoderma*, 103:203-229.

Inkpen, R. J., W. Duane, J. Burdett, and T. Yates. 2008. Assessing Stone Degradation Using an Integrated Database and Geographical Information System (GIS). *Environmental Geology*, 56: 789-801.

John, D. M., B. A. Whitton, and A. J. Brook. 2002. "The Freshwater Algal Flora of the British Isles: An Identification Guide to Freshwater and Terrestrial Algae." Cambridge University Press, Cambridge, UK.

Macedo, M. F., A. Z. Miller, A. Dionisio, and C. Saiz-Jimenez. 2009. Biodiversity of Cyanobacteria on Monuments in the Mediterranean Basin: An Overview. *Microbiology*, 155: 3476-3490.

Samad, L.K., and S.P. Adhikary. 2008. Diversity of Micro-Algae and Cyanobacteria on Building Facades and Monuments in India. *Algae*, 23:91-114.

Rindi, F. 2007. “Diversity, Distribution and Ecology of Green Algae and Cyanobacteria in Urban Habitats.” In *Algae and Cyanobacteria in Extreme Environments*, ed. J. Sechbach, pp.619-638, Dordrecht, The Netherlands: Springer.

Thornbush, M., and H. A. Viles, H.A. 2006. Changing Patterns of Soiling and Microbial Growth on Building Stone in Oxford, England After Implementation of a Major Traffic Scheme. *Science of the Total Environment*, 367:203-21.

Tomaselli, L., G. Lamenti, and P. Tiano. 2002. Chlorophyll Fluorescence for Evaluating Biocide Treatments against Phototrophic Biodeteriogens. *Annals of Microbiology*, 52: 197-206.

APPENDIX

Location of the samples taken from the NMAI building for analyses

Carol Grissom and A. Elena Charola
Museum Conservation Institute, Smithsonian Institution

The samples were collected in April 2010, upon the occasion of the visit by the four invited scientists for their further analysis. Four samples were collected and subdivided into the specimens that the scientist subsequently analyzed.

Sample #2, a fairly large spalling flake with overall black surfaces on both front and back, was readily detached from the lowest course of the loading dock wall on the west side of the building. The sample area receives rainwater from sloping capstones without any overhang; some rainwater also splashes up from the black granite ledge below (Figure 1).

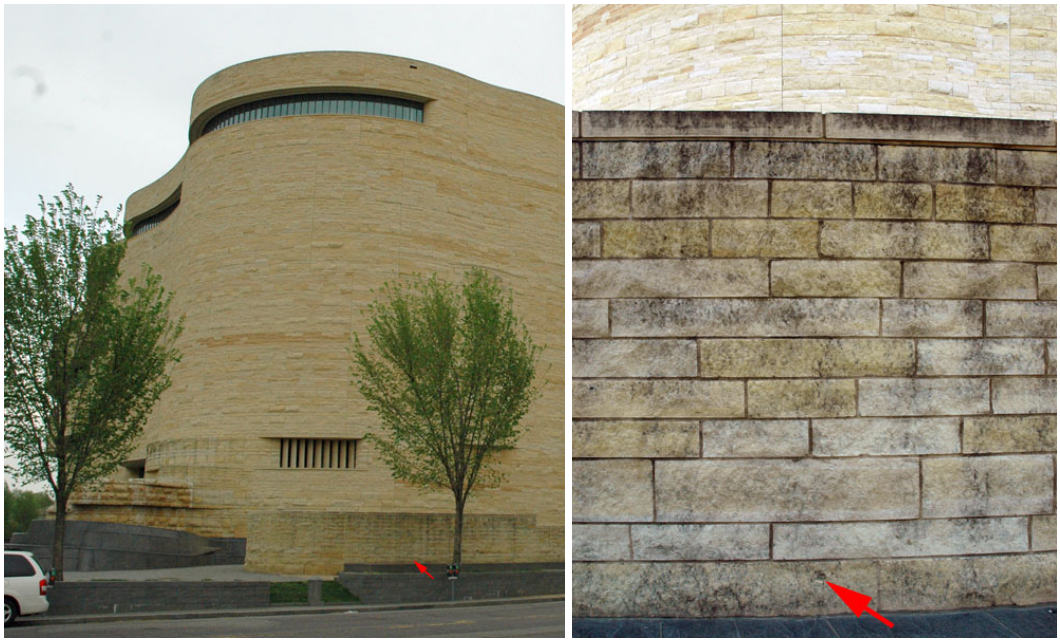

Figure 1. Sample #2 location indicated by arrows: left, general view of the exterior loading dock wall; right, detail (April 2010).

Samples #5, #7, and #9 were taken from areas of heavy biocolonization on the fifth floor terrace east wall below scuppers that drain the roofs above (Figure 2). Samples #5 and #7 were spalling flakes easily detached from below the same scupper: #5 from an area with a uniform black deposit and sample #7 from a slightly recessed area on an adjacent block with spotty surface biocolonization (Figure 3L). Sample #9 was scraped from dense black material on a membrane below a second scupper (Figure 3R).

Figure 2. Left, view of the east face of the 5th floor terrace showing locations of samples #5, #7, and #9 from darkened areas below two scuppers, which drain water from the small terrace above and, in turn, the main roof terrace with the dome (April 2010).

Figure 3. Details of sample locations shown in the previous figure. Left, samples #5 and #7 were flakes detached from areas indicated by the arrows. Note the uniform black colonization where sample #5 was taken, compared to the spotty area to its right where sample #7 was removed; right, sample #9 was scraped from the membrane at the bottom of the wall (April 2010).

The larger samples studied by May and Warscheid were pieces cut from extra blocks left over from the construction of the building.